Egypt. J. Chem. **Vol. 67**, No. 2 pp. 587 - 600 (2024)

Egyptian Journal of Chemistry

http://ejchem.journals.ekb.eg/

Antibacterial Effect of Myco-synthesized Nano-silver against Multidrug-resistant Bacteria

Nada H. Ghazala [1*], Attiya H. Mohamedin[1], Mohamed O. Abdel-Monem [2], Ashraf Elsayed [1]

[1] *Botany Department, Faculty of Science, Mansoura University, Egypt*

[2] *Botany Department, Faculty of Science, Banha University, Egypt*

Abstract

Multidrug resistance bacteria (MDR) are a serious and increasing public health problem. For controlling pathogen growth, new strategies such as biosynthesized nanoparticles by *Fusarium oxysporum* extract are urgently needed. The biosynthesis of silver nanoparticles (AgNPs) as an antibacterial agent against MDR clinical isolates bacteria such as *Staphylococcus aureus* and *Klebsiella pneumonia* was determined. Characterization of AgNPs by UV–Vis, SEM, EDAX, TEM, and SAED, Zeta potential, and antibacterial activity was performed. UV–Vis spectrum of the aqueous medium containing AgNPs showed an absorption peak at around 438 nm. TEM images detected the spherical AgNPs shape with a size ranging from (6.51-58 nm). SAED pattern study confirmed the crystalline structure of AgNPs. In this study, synthesized AgNPs exhibited strong antibacterial activity against MDR (*S. aureus* and *k. pneumonia*). Protein banding profile and RAPD PCR of *S. aureus* and *k. pneumonia* using different RAPD primers showed a strong effect of AgNPs on the genome of the tested bacteria. In conclusion; AgNPs could be an effective antibacterial agent against MRD bacteria.

Keywords: Endophytic fungi; Silver nanoparticles; MDR Bacteria; RAPD PCR.

1. Introduction

Global public health is at risk due to bacterial resistance to antibacterial agents (like antibiotics). If a bacterium stands against several drugs or carries several resistance genes, it is called a multi-resistant bacterium [1]. Antibiotic use at the peak of the outbreak was strongly linked with the pattern of antibiotic resistance in microorganisms. Resistance affects the ability to treat the infection negatively, as well as the cost and duration of the treatment [2, 3]. There is an urgent need for novel medications and alternatives because antibiotic resistance currently affects all known classes of natural and synthetic compounds. However, due to the high costs and difficulties involved in drug research and development, relatively few new antibiotics have been developed in the previous 40 years.

As a result, it is essential to continue looking for new antimicrobial agents or ways to improve those that are presently on the market [4-6]. Compared to their bulk equivalent, which can be used for bio applications, nanotechnology provides a good platform for changing the physical and chemical properties of many materials.

Nano-medicine, a branch of nanotechnology, has made strides in disease detection, monitoring, drug delivery, and control [7-9]. The process of making particles in the nanometer range, or between 1 and 100 nm, is known as nanotechnology [9-11].

Microorganisms have been used to examine potential bio-factories for the production of metallic nanoparticles such as cadmium, sulphide, gold, and silver [12]. Many types of microorganisms have been used to synthesize nanoparticles such as bacteria, fungi, and algae. Due to their antibacterial qualities, silver nanoparticles (AgNPs) are used in a variety of products, including apparel, pharmaceuticals, medical devices, and water purification systems. In addition,

*Corresponding author e-mail: nada89_hosni@yahoo.com.; (Nada H. Ghazala)
Received date 26 May 2023; revised date 07 July 2023; accepted date 31 July 2023
DOI: 10.21608/ejchem.2023.213575.8023

they are also used to adsorb metals and pesticides [13-15]. These are attributed to their unique physicochemical and biological characteristics. The growth of bacteria, viruses, and other eukaryotic microorganisms is inhibited by silver nanoparticles (AgNPs) [16, 17, and 60]. In addition to having unique qualities, their production costs are generally modest [18-21]. The use of biosynthetic techniques as an alternative to chemical and physical techniques has been studied.

Biosynthesized nanoparticles are inexpensive, dependable, and biocompatible [22, 23, and 24]. Applications for biologically produced AgNPs are likely to be numerous. There have been reports of many fungus genera producing metal nanoparticles [25-26]. Studies have demonstrated that silver nanoparticles target bacteria by attaching and breaking the cell wall, which leads to the primary structural alteration in membrane shape. This causes a large increase in membrane permeability and changes transport via the plasma membrane, both of which lead to cell death. Therefore it can be said that silver nanoparticles could be used as an alternative to antibiotics and to control microbial infections caused by MDR organisms [7, 27-29].

The present study was carried out to identify the ideal conditions for the synthesis of biogenic AgNPs using an endophytic *F. oxysporum* filtrate and to characterize it. Other objectives included testing the antibacterial effectiveness and stability of the produced AgNPs against multidrug-resistant microorganisms.

2. Materials and methods

2.1. Isolation of endophytic fungi:

Endophytic fungi *F. oxysporum* were provided from the unit of mycology, Faculty of Science, Mansoura University, Egypt to test the synthesis of AgNPs. It was isolated according to Merchant *et al* from stems of infected tomatoes [30]. Isolates were cultured and purified on a PDA medium (potato dextrose agar). Place (5–6 discs) on PDA media (potato extract 200 ml, glucose 20g, agar 15g, distilled water up to 1L) at 25°C for five days to allow the fungus to form, then move fungus to new PDA media for seven days at 25°C. To use the isolated fungus in the biosynthesis process then it was kept at 4 °C [31].

2.2. *Collection of samples and isolation of MDR bacteria:*

Multidrug-resistant bacteria used in this study Gram-positive *(Staphylococcus aureus)* and Gram-negative *(klebsiella pneumoniae)* were provided by the Clinical Microbiology Laboratories, Faculty of Medicine, Mansoura University, Egypt. Each sample was cultured and isolated on a specific medium. The Kirby Baure disc diffusion method was utilized with the Antibiogram (antibiotic sensitivity test) [32].

2.3. Biosynthesis of AgNPs by F. oxysporum:

Biomass of *F. oxysporum* was obtained by culturing 6 mm fungal discs in 500 ml Erlenmeyer flasks, which contain 3 fungal discs in 100 ml of MGYP media (Malt extract 3g, Glucose 10 g, Yeast extract 3g, and Peptone 5g) at 28°C and 180 rpm for 72 h. Filtration was used to remove the fungal mycelia, which were then thoroughly cleaned 3 to 5 times using sterilized distilled water. 20 g of the fungal biomass in 100 ml sterilized water was incubated at the same previous condition for 24 h. after filtration with Whitman filter paper. The cell-free filtrate is collected then, 1 mM $AgNO_3$ was added to it. Silver nitrate was purchased from sigma pharmaceutical industries Pharmaceutical Company.

2.4. Characterization of AgNPs

2.4.1. Ultraviolet-visible spectrophotometer analysis:

By using a UV-vis spectrophotometer, the production of the reduced AgNPs in colloidal solution was observed (Unicam UV-VIS. Spectrometer UV2, U.S.A). The supernatants' absorbance spectra were recorded between 300 and 700 nm which includes the nano-silver specific absorption range 400-450 nm [33].

2.4.2. Scan Electron microscope (SEM):

A fine powder of AgNPs was employed to look at the surface of the biosynthesized AgNPs. SEM microscope was used to capture the images (Nova Nano-SEM 450, USA) at an accelerating voltage of 20 kV. Using the Energy Dispersive X-Ray (EDX) coupled with an SEM, the elemental composition of AgNPs was analyzed [34].

2.4.3. Transmission electron microscopy (TEM):

Samples of the synthesized nano-silver were captured by TEM this was done by using standard copper with a carbon coating TEM grid was used (Type G 200, 3.05 µ diameter, TAAP, U.S.A). The sample was using TEM (JEOL JEM-2100) working at 160 k.v. Several images were taken to obtain sufficient representations of the shape and size of the synthesized nano-silver particles [34].

2.4.4. Selected area electron diffraction (SAED) pattern:

A transmission electron microscope can be used to conduct the crystallographic experimentation known as "selected area diffraction". This investigation needs a thin sectioned specimen with a thickness of around 100 nm and a high energy electron volt (100-400 k.ev). As a result, in this case, electrons will interact with the material under analysis as a wave rather than a particle. SAED pattern is the preferred method for crystalline structure analysis.

2.4.5. Zeta potential study:

To analyze the stability of nano-colloidal solutions, a zeta potential analyzer (Malvern Zeta size Nano-zs90, U.S.A.) was utilized. The zeta potential is the potential difference between the stationary fluid layer attached to the surface of the dispersed particle and the dispersion medium. The solution becomes resistant to aggregation when the zeta potential is high (Negative or Positive). This is because the repulsive force between the particles increases. The attraction between the particles overcomes the repulsion when the value is low, which causes aggregation and reduces stability [35].

2.5. Determination Minimum inhibitory concentration (MIC) of myco-synthesized AgNPs:

To estimate the lowest concentration that can prevent the apparent growth of G+ve bacteria (*S. aureus*) and G-ve bacteria (*K. pneumoniae*) were treated with increasing concentrations of AgNPs (2.5 µg/ml, 5 µg/ml, and 10 µg/ml) and incubated for 24 h at 37 ◦C. The effect of different concentrations of nano-silver precipitated on the growth (OD600) of these bacteria was measured.

2.6. Antibacterial activity of myco-synthesized AgNPs:

AgNPs' antibacterial activity against MDR bacteria like *K. pneumoniae* and *S. aureus* was performed utilizing the disc diffusion method following Minimum Inhibitory Concentration (MIC) tests. Plates with nutrient agar media were made, sterilized, and solidified. On these plates, bacteria were swabbed after they had solidified. AgNPs-only filter paper discs, Ceftriaxone-only filter paper discs, and AgNPs and Ceftriaxone filter paper discs were all placed in nutrient agar plates and incubated for 24 h at 37°C. There were measured zones of inhibition.

2.7. Transmission electron microscopy (TEM) of treated MDR bacteria by AgNPs:

According to the result of MIC and disc diffusion method of AgNPs, It is illustrated the TEM images of *k. pneumoniae* and *S. aureus* bacteria which were treated with AgNPs and their control without AgNPs.

2.8. Molecular characterization of the treated MDR bacteria with AgNPs:

Bacterial genomes were isolated from *k. pneumoniae* and *S. aureus* bacteria which were treated with AgNPs and it was fixed with electrophoresis in 1% agarose gel containing ethidium bromide and controlled by the guide of the extraction kit (Gene Jet DNA Miniprep Kit).

2.8.1. RAPD- PCR assay:

Six rapid Primers were used to investigate the effects of AgNPs on *k. pneumoniae* and *S. aureus* in Table 1. To perform the reaction PCR, the following components were created to replicate samples in a volume of (20 µL) containing the reaction PCR at the following concentrations: 4 µL DNA template, 4 µL 5x buffer, 0.5 µL Tag, 2 µL of primer and 9.5 µL water (nuclease-free). The samples were gently vortexed and the PCR was carried out under the thermal cycling conditions having the annealing temperature. After mixing these ingredients, they were placed in a thermocycler with the following schedule: The initial denaturation of template DNA at 95 ° C for 5 minutes. This was followed by 35 cycles of reaction PCR, and was as follows: At 95 ° C for 1 minute for denaturation of template DNA strands, at 30 ° C for 30 seconds to connect the primers to the template strand, at a temperature of 72 ° C for 2 minutes for polymerization of the new strand of the template strand. Then, 5 minutes was used to complete the

polymerization of incomplete strands. After optimizing the conditions of PCR, these compositions and temperature profiles were used for all primers [36].

2.8.2. SDS-PAGE for the protein of the treated MDR bacteria with AgNPs:

The *K. pneumoniae* and *S. aureus* were cultivated in LB media with AgNPs overnight at 37°C. Total protein was extracted using liquid nitrogen from AgNPs-treated MDR bacteria pellets in 100 mM phosphate buffer at pH 7 and then the Bradford technique was used to measure the protein concentration and to prepare for loading onto an acrylamide gel, 10 g of protein concentrations from each sample were boiled for 2 min in 2x sample buffer (10 mL distilled water, 2.5 mL tris-HCl, pH 6.8, 2 mL glycerol, 4 mL 10% SDS, and 1 mL -mercaptoethanol). According to Laemmli, acrylamide gel was created from two layers: a stacking gel (4%) on top of a separating gel (12%). After two hours of electrophoresis at 100 v, the gel was overnight stained with Coomassie brilliant blue R250 before being destained with a destaining solution and left to shake. The gel was recorded and examined using a program called a gel analyzer [37].

Table (1): Primer sequences used for Rapid PCR identification

Primer Name	Nucleotide sequences of primers	Annealing temperature ° C	References
U16-25	5' CTGCGCTGGA 3'	30	https://www.genelink.com
T16-25	5' GGTGAACGCT 3'	30	https://www.genelink.com
K02-25	5' GTCTCCGCAA 3'	30	https://www.genelink.com
I17-25	5' GGTGGTGATG 3'	30	https://www.genelink.com
OPB-15	5' GGAGGGTGTT 3'	32	https://www.genelink.com
OPA-11	5' CAATCGCCGT 3'	32	https://www.genelink.com

3. Results

3.1. Myco-synthesized of AgNPs:

The tested endophytic *F. oxysporum* was cultured in Maltose Glucose Yeast Peptone (MGYP) broth medium for the production of fungal biomass. Comparing the fungal biomass's growth to that of the control flask's (MGYP growth medium), which is yellowish, reveals that the fungus is growing in a reddish color as shown in Fig. 1. After incubation of *F. oxysporum* biomass with deionized water and further incubation of cell-free filtrate with 1mM silver nitrate ($AgNO_3$), the filtrate changed to dark brown color after 27 h in Fig. 2. This indicates the gradual reduction of silver ions into AgNPs.

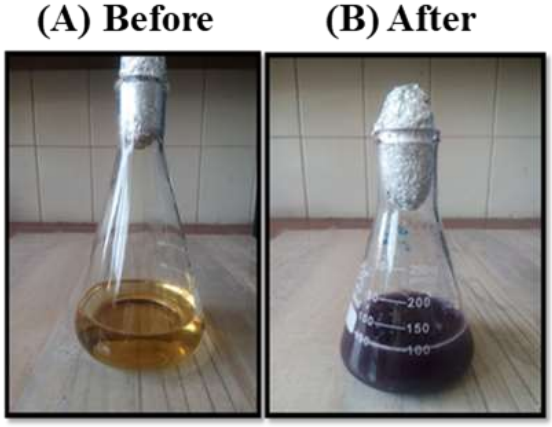

Fig. 1: The growth of *F. oxysporum* in MGYP medium. The control flask of *F. oxysporum* in (MGYP media without inoculum) is shown in (A), and a flask with biomass is shown in (B) which has the fungus's characteristic reddish color**.**

Fig. 2: Fungal cell-free filtrate with silver nitrate before incubation (A) and after incubation for 72 h (B) which changed to dark brown color by treatment with silver nitrate.

3.2. Characterization of AgNPs:

3.2.1 Ultraviolet-Visible Spectral Studies:

Nano solution was exposed to UV-VIS spectrum studies for screening to the best absorbance peak in the nano-silver specific range (350-500 nm), so the characteristic peak at 438 nm was recorded in Fig. 3. At this characteristic wavelength, the electron of conduction band makes strong oscillation to give its characteristic brown color that distinguishes nano-sized particles from macro-sized particles.

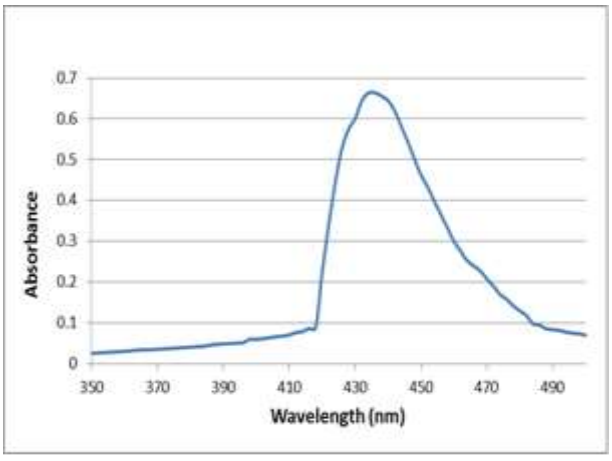

Fig. 3: UV-Vis spectrum of Myco-synthesized AgNPs which have a characteristic peak at 438 nm.

3.2.2 Scanning Electron Microscopy of AgNPs:

The crystallinity, size, and shape of the nanoparticles were characterized by scanning electron microscopy; nano-silver was a spherical or oval shape size (less than 100 nm) as shown in Fig. 4.

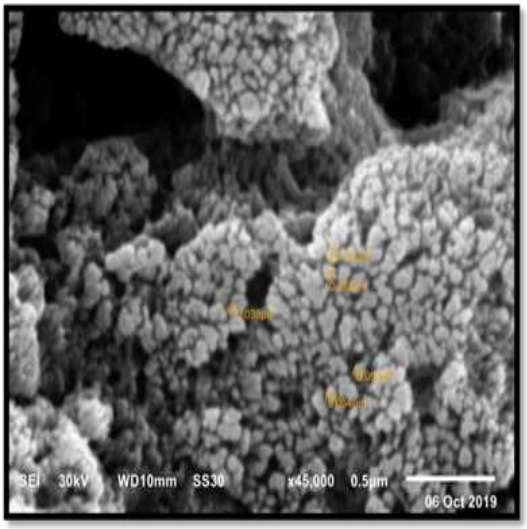

Fig.4: SEM Microscopy of biosynthesized AgNPs (less than 100 nm).

3.2.3 Transmission Electron Microscopy (TEM) analysis:

TEM image demonstrates the presence of both individual and tiny aggregated particles in the range (6.51-58 nm); the capping agent of the fungal cell-free filtrate proteins surrounds the AgNPs and keeps them from contacting one another even within aggregates. The repulsion force between the particles is caused by this capping agent. Most of the AgNPs visible in the micrograph were spherical or oval as shown in Fig. 5.

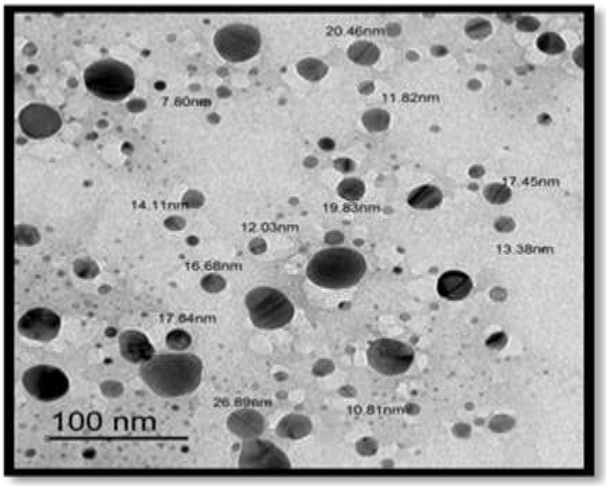

Fig. 5: TEM micrograph of Myco-synthesized of AgNPs, it's showed spherical and oval-shaped of AgNPs.

3.2.4 Selected Area Electron Diffraction (SAED) Pattern Analysis of AgNPs:

When a single drop of nano-colloidal fluid was treated to SAED analysis, the diffraction pattern of the nano-silver particles appeared as bright dots on the

dark field. This diffraction pattern confirms the fabrication of nano-silver by reflecting the crystalline structure and diffraction rings of nano-silver Fig. 6.

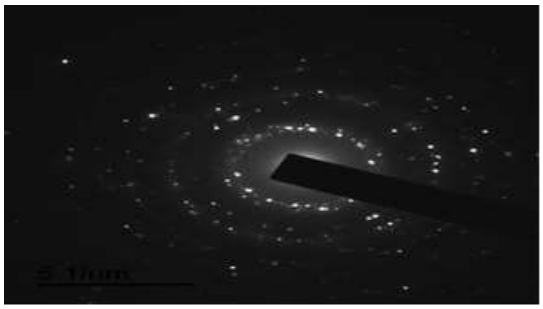

Fig. 6: This micrograph of the SAED pattern for one nano-silver particle revealed that silver atoms, which appeared as light spots, were present in the diffraction rings.

3.2.5 Zeta potential analysis:

Zeta potential analysis is utilized to measure the stability and surface charge of a nano-colloidal solution, the zeta potential measurement of the synthesized AgNPs is depicted in Fig. 7. The value of Zeta potential of AgNPs -17.7 mV indicates the stability of the nano-silver. Additionally, the conductivity, which is 0.173, shows that the produced AgNPs are stable and homogeneous.

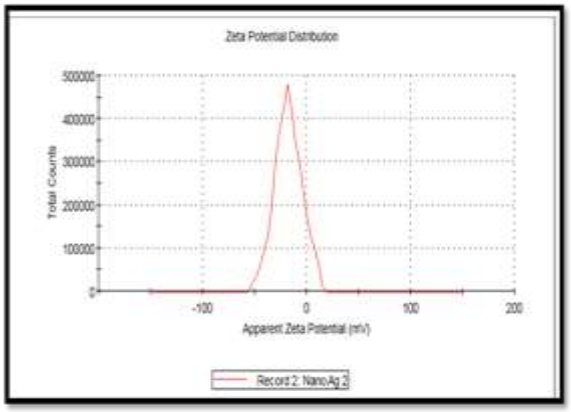

Fig. 7: Zeta potential of AgNPs.

3.2.6 Energy dispersive analysis of X-ray (EDX):

The EDX spectrum is recorded in the spot-profile mode as shown in Fig. 8. The optical absorption peak is observed at 3.0 KeV, which is typical for the absorption of metallic AgNPs. Strong signals from the silver atoms were observed, while weaker signals from O, Cl, Ca, Cu, and Zn atoms are also recorded. From the EDX spectrum, it is clear that nano-silver reduced by *F. oxysporum* has the weight percentage of silver as 70.76% as shown in Table. 2.

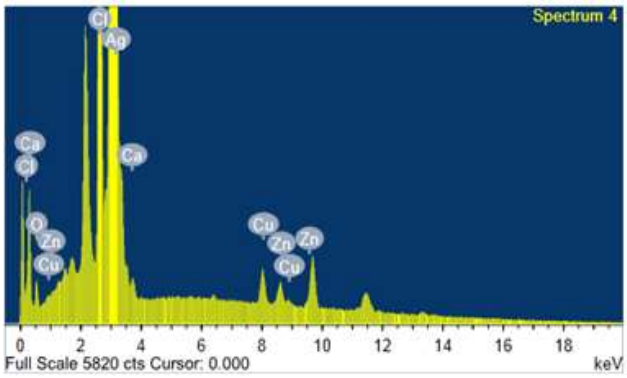

Fig. 8: EDX spectrum of the biosynthesized AgNPs.

Table 2: The element composition of the AgNPs of EDX spectra

Elment	Weight%	Atomic%
O	7.04	42.82
Cl	22.75	62.45
Ca	0.7	1.87
Cu	3.1	4.85
Zn	1.9	2.88
Ag	78.4	70.76

3.3 Determination of AgNPs MIC its and antibacterial activity:

The multidrug-resistant bacteria; *S. aureus* and *K. pneumoniae* were used in this study to determine the antimicrobial effect of AgNPs using disc diffusion and broth dilution techniques. The antibiogram, often known as an antibiotic sensitivity test, was carried out using the Kirby Baure disc diffusion method [32]. The isolates, recorded resistance to tested antibiotics (Ceftazidim, Cefaclor, Meropenem, Trimethoprim, Ampicillin/sulbactam, Imipenem, Ciprofloxacin, and Amikacin) as shown in Fig. 9.

All investigated bacteria' growth was fully inhibited by the AgNPs precipitate at a concentration of 10 µg/ml (Table 3). On the other hand, the two other tested concentrations of AgNPs (5µg/ml and 2.5µg/ml) did not completely stop the growth of the examined organisms. By disc diffusion method to check the antimicrobial activity of the AgNPs according to the result of MIC assays and Comparison of Ceftriaxone antibiotic.

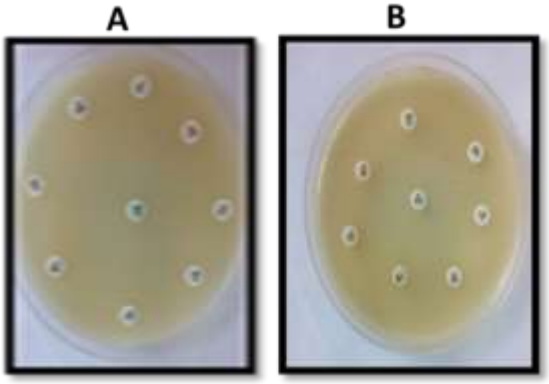

Fig. 9: Multidrug-resistant bacteria; (A) *S.aureus* and (B) *K. pneumoniae* with different antibiotic disks.

The results of the inhibition zone study showed in Table. (4) and Fig. (10). The AgNPs have a great potential effect than Ceftriaxone as standard antibacterial agents for Gram-positive and Gram-negative. It was found that the increased inhibition zone diameter in the case of AgNPs with antibiotic mixtures.

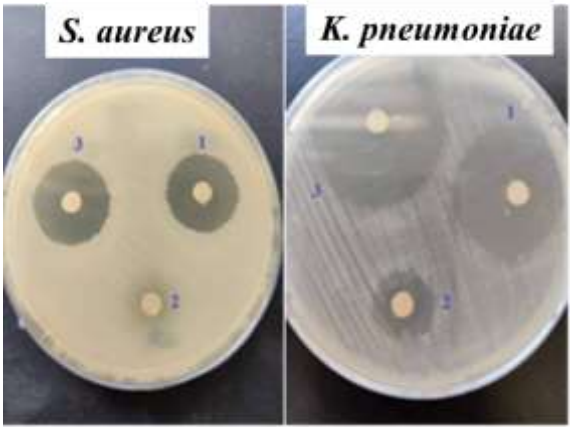

Fig. 10: Antibacterial activity of AgNps in comparison to Ceftriaxone antibiotic on Muller Hinton agar by disc diffusion method for multidrug-resistant bacteria (*K. pneumoniae* and *S. aureus*). Number (1) is silver nanoparticles (AgNps), number (2) is Ceftriaxone, and number (3) is a mixture of (AgNps) with Ceftriaxone.

Table 3: Showed the MIC of AgNPs on microbial growth.

MDR bacteria	(MIC) µg/ml
S. aureus	10
K. pneumoniae	10

Table 4: The inhibition zone of AgNps and antibiotic

Strain	Mean zone of inhibition (mm)		
	AgNPs	Ceftriaxone	AgNPs + Ceftriaxone
S. aureus	20	2	25
K. pneumoniae	30	5	35

3.4 Ultrastructure of the treated MDR bacteria by (TEM):

Fig. 11 and Fig. 12 illustrated the TEM images of *K. pneumoniae* and *S. aureus* treated with AgNPs. It showed the structure of a cell in its unaltered state without the use of AgNPs (control) and additionally demonstrated a disrupted cell membrane, cytoplasm leakage from the outside of the cell into it, internal AgNP deflection, and thick patches in the cytoplasm. Additionally, protoplasmic shrinkage, cellular membrane separation, and cell rupture and disintegration were noted.

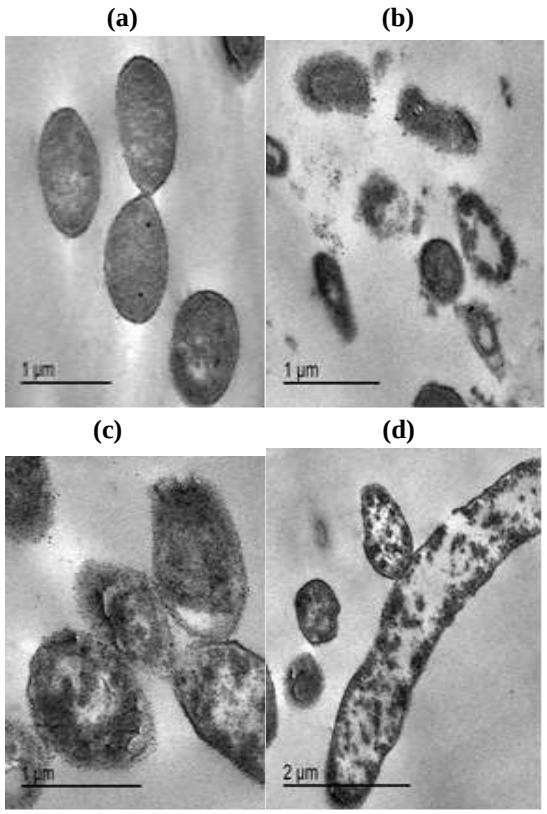

Fig. (11): Changes in *K. pneumoniae* cell structure observed by TEM, with or without AgNPs. (a) Is the structure of an intact cell (control) but the cell membrane is destroyed, the cytoplasm is released, there are dense patches inside the cytoplasm, the cell disintegrates, the protoplasm shrinks, and the cell membrane separates (cellular deformation) in (b,c, and d).

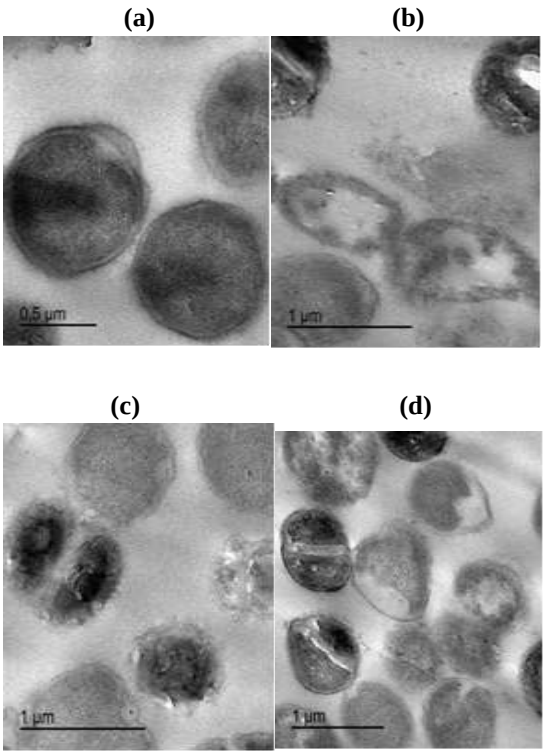

Fig. 12: TEM morphological alterations in the cell structure of *S. aureus* with or without AgNPs. (a) is intact cell structure (control) but the separation of the cellular membrane, release of the cytoplasm, dense areas within the cytoplasm, cellular disintegration, shrinkage of the protoplasm, and cellular disintegration (cellular deformation) in (b, c, and d).

3.5 Molecular characterization of the treated MDR bacteria:

3.5.1 Effect of AgNPs on DNA of MDR bacteria

The genomic DNA of the treated MDR *(S. aureus) and (K. pneumoniae)* before and after treatment with AgNPs was larger than 10 Kb **Fig**. **13**.

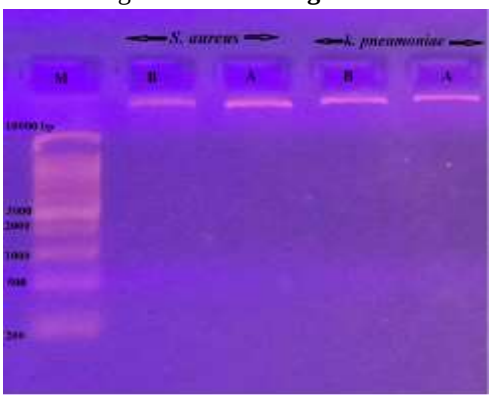

Fig. 13: Bacterial genomic DNA of multidrug resistance bacteria **(*S. aureus* and *K. pneumoniae)*** before (B) and after (A) treatment of AgNPs. **(M)** is 1 Kb DNA ladder on 1% agarose gel.

The electrophoretic bands were obtained from the amplification of random sequences of genomic DNA (gDNA) from the tested bacteria (S. aureus and k. pneumoniae) with AgNPs using 6 RAPD primers listed in Table.1. RAPD Primers were categorized into two groups 1 and 2, three primer in each group. The polymorphic bands exposed from electrophoresis showed a high effect of AgNPs on (gDNA) according to the presence or absence of the bands. The RAPD profile of the DNA through agarose gel electrophoresis shows variations in the intensity of bands Fig. 14.

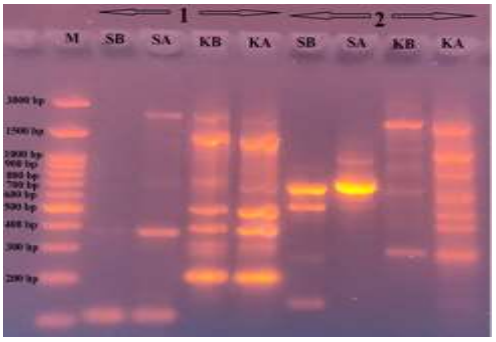

Fig. 14: RAPD gel documentation of (*S. aureus* and *K. pneumoniae*) before (B) after (A) treatment with AgNPs amplified by a mixture of two groups of primers (1 and 2) three primers in each group. (M) is the DNA marker.

3.5.1 Effect of AgNPs on protein profile of MDR bacteria:

The protein banding profile of the multidrug-resistant bacteria in the presence of AgNPs was depicted in Fig. 15. Analysis of the protein banding pattern of S. aureus and *K. pneumoniae* grown on LB containing AgNPs, Table 5 showed that the total protein bands recorded on 27 bands distributed as; 18 monomorphic bands that haven't altered in the protein pattern and seem like the control bands, 6 unique and 3 polymorphic bands. In Fig. 15, there are many bands present only in control but disappeared after treatment of AgNPs such as bands with molecular mass 147 and 87 kDa in S. aureus and 129 KDa in *k. pneumoniae* this indicated by (red arrows). The molecular mass of the new two bands (35.8 and 32 kDa) was raised in *K. pneumoniae* (black arrows).

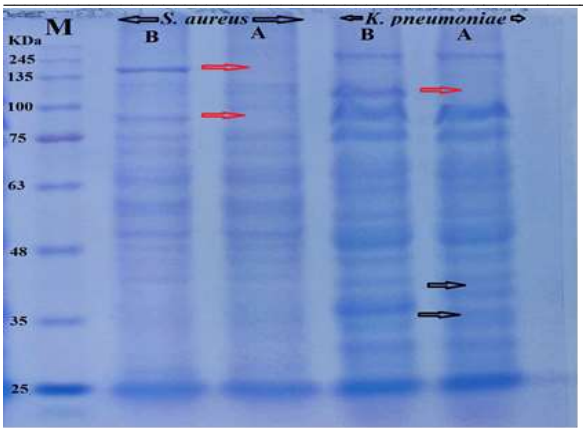

Fig. 15: Protein profile MDR bacteria *S. aureus* and *K. pneumoniae* cultured on LB media separated on 14% acrylamide (B) and after (A) treatment with AgNps. The first lane (M) is the protein ladder. New bands are denoted by a black arrow, while bands that have disappeared bands are indicated by a red arrow.

Table 5: Gel analysis of protein pattern of MDR bacteria *S. aureus* and *K. pneumoniae* before (A) and after (B) treatment with AgNPs.

No. of band	The molecular weight of bands	Polymorphism	RF	*S. aureus*		*K. pneumoniae*	
				A	B	A	B
1	159.611	Polymorphic	0.091	-	-	+	+
2	147.981	Unique	0.124	+	-	-	-
3	129.855	Polymorphic	0.181	+	+	-	-
4	129.557	Unique	0.182	-	-	+	-
5	112.65	Polymorphic	0.243	-	-	+	+
6	109.845	Unique	0.254	+	-	-	-
7	98.851	Monomorphic	0.3	+	+	+	+
8	87.743	Monomorphic	0.352	+	+	+	+
9	79.689	Monomorphic	0.394	+	+	+	+
10	76.117	Monomorphic	0.414	+	+	+	+
11	70.734	Monomorphic	0.446	+	+	+	+
12	66.641	Monomorphic	0.472	+	+	+	+
13	61.362	Monomorphic	0.508	+	+	+	+
14	58.612	Monomorphic	0.528	+	+	+	+
15	56.114	Monomorphic	0.547	+	+	+	+
16	52.025	Monomorphic	0.58	+	+	+	+
17	48.346	Monomorphic	0.612	+	+	+	+
18	45.132	Monomorphic	0.642	+	+	+	+
19	42.913	Monomorphic	0.664	+	+	+	+
20	38.003	Unique	0.717	-	-	-	+
21	35.804	Unique	0.743	-	-	+	-
22	34.043	Monomorphic	0.765	+	+	+	+
23	32	Unique	0.792	-	-	-	+
24	28.666	Monomorphic	0.84	+	+	+	+
25	25.975	Monomorphic	0.883	+	+	+	+
26	23.753	Monomorphic	0.922	+	+	+	+
27	21.573	Monomorphic	0.964	+	+	+	+
No. of bands/lane				21	19	22	22
Total No. of bands						27	
No. of monomorphic bands						18	
No. of unique bands						6	
No. of polymorphic bands						3	

4. DISCUSSION

One of the biggest health issues is the rise of serious bacterial antibiotic resistance. Through the inadequate treatment of bacterial infections, multidrug-resistant bacteria have emerged [38]. Nanoparticles are considered as novel antibacterial agents. Recently, both academic and commercial sectors have become more interested in the creation of environmentally safe antimicrobial nanoparticles such as silver nanoparticles with unique physical, chemical, and biological characteristics. Synthesizing silver nanoparticles using the biological method increased their antimicrobial activity [39, 40].

In this study, *F. oxysporum* extract reduced silver nitrate ions forming AgNPs along with color changing from light brown to dark brown. Several previous studies on the biosynthesis of AgNPs by *F. oxysporum*, *P. aeruginosa*, and yeast by the extracellular process were reported. Additionally, it has been shown that this enzyme can be used to create AgNPs *in vitro* under anaerobic conditions [41-43].

UV-visible spectroscopy was used in this study to analyze the generated AgNPs where a high, broad peak was observed between 350 and 500 nm in the UV-VIS absorption spectra, with the distinctive peak being measured at 438 nm. In a different study, silver nanoparticles synthesized by *Candida utilis* and *Kluyveromyces marxianus* showed a strong, broad peak in the UV-vis absorption spectra between 430 and 450 nm and 400 and 430 nm, respectively [41, 44].

Scanning electron microscopy was used in this study to examine the surface morphology of artificial nanoparticles. The scanning electron image of silver nanoparticles synthesized by *F. oxysporum* at a magnification of 45,000 x showed the size of the silver nanoparticles resembled a spherical and less than 100 nm. In other studies, a scanning electron micrograph of silver nanoparticles from *Murraya koenigii* was displayed [45]. The majority of silver nanoparticles were also spherical with a smooth surface, less than 100 nm in size, and individual and aggregated nanoparticles [46, 61].

The size and shape of the nanoparticles were visible in the most recent data from transmission electron microscopy. This micrograph demonstrates the existence of both aggregated and isolated particles in the range of 6.5-58 nm. The Nano-silver that appeared

in the micrograph was mostly spherical or oval. In other studies, the particles from *Candida utilis* were spherical in the range of 6-20 nm and uniformly distributed without significant agglomeration of AgNPs [47, 48].

Lighted patches on the shadowy field represented the AgNPs particle diffraction pattern. AgNPs' crystalline structure and diffraction rings are reflected in this pattern, which serves as a confirmation of the synthesis of AgNPs. The diffraction pattern from the chosen area in another investigation supports metallic silver's face-centered cubic crystalline structure [49].

To determine the stability and surface charge of a nano-colloidal solution, a zeta potential analyzer is used. The stability of the AgNPs is indicated by their -17.7mV zeta potential in this investigation. Additionally, the conductivity, which is 0.173, shows that the produced AgNPs are stable and homogeneous. The biosynthesized AgNPs' zeta potential was discovered to have a high peak at -7.66 mV in another investigation. It is hypothesized that the nanoparticles' surfaces are negatively charged and diffused throughout the liquid. The fact that it is negative demonstrates that the particles repel one another and that they are extremely stable [50, 51].

The optical absorption peak in the EDX analysis at 3.0 KeV, is characteristic for the absorption of metallic nano-silver. Weak signals from O, Cl, Ca, Cu, and Zn atoms are also recorded and including strong signals from the silver atoms. From the EDX analysis, it is clear that nano-silver reduced by *F. oxysporum* has the weight percentage of silver as 70.76%. Also, the production of silver nanoparticles was observed in the 3.0 keV regions and exhibits a typically big signal peak because surface plasmon resonance has been reported previously by [52, 53].

The antibacterial effect of AgNPs was investigated in the current study on various types of multidrug-resistant bacteria such as *k. pneumoniae* as Gram-negative and *S. aureus* as Gram-positive bacteria. The concentration of AgNPs at 10 µg/ml has inhibited the growth of all bacteria by minimum inhibitory concentration (MIC). However, the two other nano-silver concentrations 5 µg/ml and 2.5 µg/ml could not completely stop the growth of the tested bacteria. As typical antibacterial medicines for Gram-positive and Gram-negative bacteria, the findings of the inhibitory investigation demonstrated that AgNPs have a greater potential impact than the standard antibiotic Ceftriaxone. AgNPs and antibiotic combinations were observed to increase the diameter of the inhibitory zones. In other investigations, seven microorganisms and three different AgNP concentrations were used to examine the antibacterial properties. The numerical value of the inhibitory zone of the control of *E. coli, K. pneumoniae* and *Shigella spp* compared to ofloxacin antibiotics were investigated and then reported [54]. The synthesized AgNPs had the most effective antibacterial agents against *E. coli* and *B. subtilis*, respectively. AgNPs exhibit less antibacterial action against k. *pneumoniae, M. flavus, P. aeruginosa, B. pumilus* and *S. aureus* [55].

The TEM micrographs of *K. pneumoniae* and *S. aureus* displayed the structure of an intact cell that had not been exposed to AgNPs (the control), as well as broken cell wall, cytoplasm leaking from the outside of the cell also dark particles or dense patches were observed in the cytoplasm. Additionally, protoplasmic shrinkage, cellular membrane separation, and cell rupture and disintegration were noted. In other studies, the mechanism of AgNPs in bacterial inactivation may be linked to damage to the cell wall and plasma membrane due to protein inactivation and peroxidation of membrane lipids, which disturbed the structural integrity of the membrane and led to transport problems and potassium leakage. The communication system of bacterial growth may be affected by silver nanoparticles within the cell by modulating the tyrosine phosphorylation of identified peptide substrates, which may cluster without any interaction between the AgNPs, suggesting its stabilization by a capping agent [56, 57].

The mixture of RAPD primers which have three primers in each group (1 and 2). The bands gotten from were scored due to the presence or absence and fewer bands appear. Also in other studies, it was done to investigate the results of silver and copper oxide nanoparticles on the genome of Escherichia coli strain O157: H7 as a model for gram-negative bacteria. In light of this, determined by the RAPD-PCR reaction with 14 primers, the presence or lack of bands in the gel indicates that silver and copper oxide nanoparticles are modifying the DNA's sequence. Numerous primers failed to identify the target sequences, which prevented the associated segments from replicating and caused the absence of bands on the agarose gel [58, 59]. The alterations in cellular protein after exposure to AgNPs were seen from gel electrophoresis results because it interferes with metabolic process and

cell wall, nucleic acid, and protein synthesis, protein pattern alteration causes bacterial death. Analysis of the multidrug-resistant bacteria's protein banding patterns after exposure to AgNPs indicated that there were 27 bands scattered overall as 18 monomorphic, 3 polymorphic bands, and 6 unique bands. Previous research revealed that AgNPs may also alter protein receptors, causing poor lipid transport and ultimately cell death [54, 59].

5. Conclusion

In conclusion, silver nanoparticles have a strong antibacterial effect on multidrug-resistant bacteria. Further experiments should be done to determine the toxicity and potential side effects of using AgNPs in the healthcare system.

6. References

1. Barbosa, T.M. and S.B. Levy, Differential expression of over 60 chromosomal genes in Escherichia coli by constitutive expression of MarA. Journal of Bacteriology, 2000. 182(12): p. 3467-3474.
2. Nathan, C. and F.M. Goldberg, The profit problem in antibiotic R&D. Nature Reviews Drug Discovery, 2005. 4(11): p. 887.
3. Elsayed, A., A. Mohamedin, T. Ata, and N. Ghazala, Molecular characterization of multidrug-resistant clinical Escherichia coli isolates. Am. J. Biochem. Mol. Biol, 2016. 6: p. 72-83.
4. Tyers, M. and G.D. Wright, Drug combinations: a strategy to extend the life of antibiotics in the 21st century. Nature Reviews Microbiology, 2019. 17(3): p. 141-155.
5. De Jong, W.H. and P.J. Borm, Drug delivery and nanoparticles: applications and hazards. International journal of nanomedicine, 2008. 3(2): p. 133.
6. Elmogy, S., M.A. Ismail, R.Y. Hassan, A. Noureldeen, H. Darwish, E. Fayad, F. Elsaid, and A. Elsayed, Biological Insights of Fluoroaryl-2, 2′-Bichalcophene Compounds on Multi-Drug Resistant Staphylococcus aureus. Molecules, 2020. 26(1): p. 139.
7. Piddock, L.J., The crisis of no new antibiotics—what is the way forward? The Lancet infectious diseases, 2012. 12(3): p. 249-253.
8. Högberg, L.D., A. Heddini, and O. Cars, The global need for effective antibiotics: challenges and recent advances. Trends in pharmacological sciences, 2010. 31(11): p. 509-515.
9. Elsayed, A., G.M. El-Shamy, and A.A. Attia, Biosynthesis, Characterization, and Assessment of Zirconia Nanoparticles by Fusarium oxysporum species as Potential Novel Antimicrobial and Cytotoxic Agents. Egyptian Journal of Botany, 2022. 62(2): p. 507-522.
10. He, Y., Z. Du, H. Lv, Q. Jia, Z. Tang, X. Zheng, K. Zhang, and F. Zhao, Green synthesis of silver nanoparticles by Chrysanthemum morifolium Ramat. extract and their application in clinical ultrasound gel. International Journal of Nanomedicine, 2013. 8: p. 1809.
11. Das, S.K., M.M.R. Khan, A.K. Guha, A.R. Das, and A.B. Mandal, Silver-nano biohybride material: synthesis, characterization and application in water purification. Bioresource technology, 2012. 124: p. 495-499.
12. Sastry, M., A. Ahmad, M.I. Khan, and R. Kumar, Biosynthesis of metal nanoparticles using fungi and actinomycete. Current science, 2003: p. 162-170.
13. Asthana, A., R. Verma, A.K. Singh, M.A.B.H. Susan, and R. Adhikari. Silver Nanoparticle Entrapped Calcium-Alginate Beads for Fe (II) Removal via Adsorption. in Macromolecular Symposia. 2016. Wiley Online Library.
14. Lin, S., R. Huang, Y. Cheng, J. Liu, B.L. Lau, and M.R. Wiesner, Silver nanoparticle-alginate composite beads for point-of-use drinking water disinfection. Water research, 2013. 47(12): p. 3959-3965.
15. Elsayed, A., K. Hashish, and A.-D. Sherief, Production and characterization OF silver nanoparticles synthesized BY nanoparticles synthesized BY FUSARIUM oxysporum FUSARIUM oxysporum. Journal of Environmental Sciences, 2015. 44(4): p. 681-691.
16. Jeong, S.H., S.Y. Yeo, and S.C. Yi, The effect of filler particle size on the antibacterial properties of compounded polymer/silver fibers. Journal of Materials Science, 2005. 40(20): p. 5407-5411.
17. Elsayed, A., Z. Moussa, S.S. Alrdahe, M.M. Alharbi, A.A. Ghoniem, A.Y. El-Khateeb, and W.I. Saber, Optimization of Heavy Metals Biosorption via Artificial Neural Network: A Case Study of Cobalt (II) Sorption by Pseudomonas alcaliphila NEWG-2. Front. Microbiol. 13: 893603. doi: 10.3389/fmicb, 2022.

18. Mandal, S., S. Phadtare, and M. Sastry, Interfacing biology with nanoparticles. Current Applied Physics, 2005. 5(2): p. 118-127.
19. Solanki, J.N. and Z. Murthy, Highly monodisperse and sub-nano silver particles synthesis via microemulsion technique. Colloids and Surfaces A: Physicochemical and Engineering Aspects, 2010. 359(1-3): p. 31-38.
20. Huang, J., G. Zhan, B. Zheng, D. Sun, F. Lu, Y. Lin, H. Chen, Z. Zheng, Y. Zheng, and Q. Li, Biogenic silver nanoparticles by Cacumen platycladi extract: synthesis, formation mechanism, and antibacterial activity. Industrial & Engineering Chemistry Research, 2011. 50(15): p. 9095-9106.
21. Wang, Z., J. Chen, P. Yang, and W. Yang, Biomimetic synthesis of gold nanoparticles and their aggregates using a polypeptide sequence. Applied Organometallic Chemistry, 2007. 21(8): p. 645-651.
22. Elamawi, R.M., R.E. Al-Harbi, and A.A. Hendi, Biosynthesis and characterization of silver nanoparticles using Trichoderma longibrachiatum and their effect on phytopathogenic fungi. Egyptian journal of biological pest control, 2018. 28(1): p. 1-11.
23. Emeka, E.E., O.C. Ojiefoh, C. Aleruchi, L.A. Hassan, O.M. Christiana, M. Rebecca, E.O. Dare, and A.E. Temitope, Evaluation of antibacterial activities of silver nanoparticles green-synthesized using pineapple leaf (Ananas comosus). Micron, 2014. 57: p. 1-5.
24. Ahmed, M. K., Menazea, A. A., & Abdelghany, A. M. (2020). Blend biopolymeric nanofibrous scaffolds of cellulose acetate/ε-polycaprolactone containing metallic nanoparticles prepared by laser ablation for wound disinfection applications. International journal of biological macromolecules, 155, 636-644.
25. Syed, A. and A. Ahmad, Extracellular biosynthesis of platinum nanoparticles using the fungus Fusarium oxysporum. Colloids and Surfaces B: Biointerfaces, 2012. 97: p. 27-31.
26. Murphy, M., K. Ting, X. Zhang, C. Soo, and Z. Zheng, Current development of silver nanoparticle preparation, investigation, and application in the field of medicine. Journal of nanomaterials, 2015. 2015.
27. Heikal, Y.M., N.A. Şuţan, M. Rizwan, and A. Elsayed, Green synthesized silver nanoparticles induced cytogenotoxic and genotoxic changes in Allium cepa L. varies with nanoparticles doses and duration of exposure. Chemosphere, 2020. 243: p. 125430.
28. Soliman, H., A. Elsayed, and A. Dyaa, Antimicrobial activity of silver nanoparticles biosynthesised by Rhodotorula sp. strain ATL72. Egyptian Journal of Basic and Applied Sciences, 2018. 5(3): p. 228-233.
29. Jung, W.K., H.C. Koo, K.W. Kim, S. Shin, S.H. Kim, and Y.H. Park, Antibacterial activity and mechanism of action of the silver ion in Staphylococcus aureus and Escherichia coli. Applied and environmental microbiology, 2008. 74(7): p. 2171-2178.
30. Raffi, M., F. Hussain, T. Bhatti, J. Akhter, A. Hameed, and M. Hasan, Antibacterial characterization of silver nanoparticles against E. coli ATCC-15224. Journal of materials science and technology, 2008. 24(2): p. 192-196.
31. Merchant, S.S., S.E. Prochnik, O. Vallon, E.H. Harris, S.J. Karpowicz, G.B. Witman, A. Terry, A. Salamov, L.K. Fritz-Laylin, and L. Maréchal-Drouard, The Chlamydomonas genome reveals the evolution of key animal and plant functions. Science, 2007. 318(5848): p. 245-250.
32. Hallmann, J., G. Berg, and B. Schulz, Isolation procedures for endophytic microorganisms, in Microbial root endophytes. 2006, Springer. p. 299-319.
33. Bauer, T.N. and B. Erdogan, Organizational socialization. APA Handbook of I/O Psychology, 1996. 3: p. 51-64.
34. Basavaraja, S., S. Balaji, A. Lagashetty, A. Rajasab, and A. Venkataraman, Extracellular biosynthesis of silver nanoparticles using the fungus Fusarium semitectum. Materials Research Bulletin, 2008. 43(5): p. 1164-1170.
35. Maines, T.R., A. Jayaraman, J.A. Belser, D.A. Wadford, C. Pappas, H. Zeng, K.M. Gustin, M.B. Pearce, K. Viswanathan, and Z.H. Shriver, Transmission and pathogenesis of swine-origin 2009 A (H1N1) influenza viruses in ferrets and mice. Science, 2009. 325(5939): p. 484-487.
36. Hanaor, D., M. Michelazzi, C. Leonelli, and C.C. Sorrell, The effects of carboxylic acids on the aqueous dispersion and electrophoretic deposition of ZrO 2. Journal of the European Ceramic Society, 2012. 32(1): p. 235-244.

37. Williams, J.G., A.R. Kubelik, K.J. Livak, J.A. Rafalski, and S.V. Tingey, DNA polymorphisms amplified by arbitrary primers are useful as genetic markers. Nucleic acids research, 1990. 18(22): p. 6531-6535.
38. Laemmli, U.K., Cleavage of structural proteins during the assembly of the head of bacteriophage T4. nature, 1970. 227(5259): p. 680-685.
39. Huh, A.J. and Y.J. Kwon, "Nanoantibiotics": a new paradigm for treating infectious diseases using nanomaterials in the antibiotics resistant era. Journal of controlled release, 2011. 156(2): p. 128-145.
40. Xie, J., J.Y. Lee, D.I. Wang, and Y.P. Ting, Silver nanoplates: from biological to biomimetic synthesis. ACS nano, 2007. 1(5): p. 429-439.
41. Ramalingam, B., T. Parandhaman, and S.K. Das, Antibacterial effects of biosynthesized silver nanoparticles on surface ultrastructure and nanomechanical properties of gram-negative bacteria viz. Escherichia coli and Pseudomonas aeruginosa. ACS applied materials & interfaces, 2016. 8(7): p. 4963-4976.
42. Saravanan, M., A.K. Vemu, and S.K. Barik, Rapid biosynthesis of silver nanoparticles from Bacillus megaterium (NCIM 2326) and their antibacterial activity on multi drug resistant clinical pathogens. Colloids and Surfaces B: Biointerfaces, 2011. 88(1): p. 325-331.
43. Jeevan, P., K. Ramya, and A.E. Rena, Extracellular biosynthesis of silver nanoparticles by culture supernatant of Pseudomonas aeruginosa. 2012.
44. Marcato, P., G. De Souza, O. Alves, E. Esposito, and N. Durán, Antibacterial activity of silver nanoparticles synthesized by Fusarium oxysporum strain. Proceedings of 2nd Mercosur Congr. on Chem. Eng., 4th Mercosur Congr. on Process Sys. Eng, 2005: p. 1-5.
45. Kathiresan, K., S. Manivannan, M. Nabeel, and B. Dhivya, Studies on silver nanoparticles synthesized by a marine fungus, Penicillium fellutanum isolated from coastal mangrove sediment. Colloids and surfaces B: Biointerfaces, 2009. 71(1): p. 133-137.
46. Jeyaraj, M., S. Varadan, K.J.P. Anthony, M. Murugan, A. Raja, and S. Gurunathan, Antimicrobial and anticoagulation activity of silver nanoparticles synthesized from the culture supernatant of Pseudomonas aeruginosa. Journal of Industrial and Engineering Chemistry, 2013. 19(4): p. 1299-1303.
47. Suman, T., S.R. Rajasree, A. Kanchana, and S.B. Elizabeth, Biosynthesis, characterization and cytotoxic effect of plant mediated silver nanoparticles using Morinda citrifolia root extract. Colloids and surfaces B: Biointerfaces, 2013. 106: p. 74-78.
48. Gole, A., C. Dash, V. Ramakrishnan, S. Sainkar, A. Mandale, M. Rao, and M. Sastry, Pepsin− gold colloid conjugates: preparation, characterization, and enzymatic activity. Langmuir, 2001. 17(5): p. 1674-1679.
49. Guzmán, M.G., J. Dille, and S. Godet, Synthesis of silver nanoparticles by chemical reduction method and their antibacterial activity. Int J Chem Biomol Eng, 2009. 2(3): p. 104-111.
50. Ibrahim, H.M., Green synthesis and characterization of silver nanoparticles using banana peel extract and their antimicrobial activity against representative microorganisms. Journal of radiation research and applied sciences, 2015. 8(3): p. 265-275.
51. Jagtap, U.B. and V.A. Bapat, Green synthesis of silver nanoparticles using Artocarpus heterophyllus Lam. seed extract and its antibacterial activity. Industrial crops and products, 2013. 46: p. 132-137.
52. Vijayakumar, M., K. Priya, F. Nancy, A. Noorlidah, and A. Ahmed, Biosynthesis, characterisation and anti-bacterial effect of plant-mediated silver nanoparticles using Artemisia nilagirica. Industrial Crops and Products, 2013. 41: p. 235-240.
53. Kaviya, S., J. Santhanalakshmi, B. Viswanathan, J. Muthumary, and K. Srinivasan, Biosynthesis of silver nanoparticles using Citrus sinensis peel extract and its antibacterial activity. Spectrochimica Acta Part A: Molecular and Biomolecular Spectroscopy, 2011. 79(3): p. 594-598.
54. Das, J., M.P. Das, and P. Velusamy, Sesbania grandiflora leaf extract mediated green synthesis of antibacterial silver nanoparticles against selected human pathogens. Spectrochimica Acta Part A: Molecular and Biomolecular Spectroscopy, 2013. 104: p. 265-270.
55. Li, W.-R., X.-B. Xie, Q.-S. Shi, S.-S. Duan, Y.-S. Ouyang, and Y.-B. Chen, Antibacterial effect of

silver nanoparticles on Staphylococcus aureus. Biometals, 2011. 24(1): p. 135-141.
56. Patel, D.K., D. Laloo, R. Kumar, and S. Hemalatha, Pedalium murex Linn.: an overview of its phytopharmacological aspects. Asian Pacific Journal of tropical medicine, 2011. 4(9): p. 748-755.
57. Shrivastava, S., T. Bera, A. Roy, G. Singh, P. Ramachandrarao, and D. Dash, Characterization of enhanced antibacterial effects of novel silver nanoparticles. Nanotechnology, 2007. 18(22): p. 225103.
58. Gopinath, V., S. Priyadarshini, M.F. Loke, J. Arunkumar, E. Marsili, D. MubarakAli, P. Velusamy, and J. Vadivelu, Biogenic synthesis, characterization of antibacterial silver nanoparticles and its cell cytotoxicity. Arabian journal of chemistry, 2017. 10(8): p. 1107-1117.
59. Fariba, A., G.E. Bahram, K. Farrokh, S. Tabrizy, and S.S. Pooneh, An investigation of the effect of copper oxide and silver nanoparticles on E. coli genome by RAPD molecular markers. J Adv Biotechnol Microbiol, 2016. 1: p. 1-6.
60. Abdelghany, A. M., et al. "Combined DFT/FTIR structural studies of monodispersed PVP/Gold and silver nano particles." Journal of Alloys and Compounds 646 (2015): 326-332.
61. Waly, A. L., A. M. Abdelghany, and A. E. Tarabiah. "A comparison of silver nanoparticles made by green chemistry and femtosecond laser ablation and injected into a PVP/PVA/chitosan polymer blend." Journal of Materials Science: Materials in Electronics 33.29 (2022): 23174-23186.